Pattern Reconfigurable Printed Antennas with High Gain and Broadband

Xue-Xia Yang, Zhong-Liang Lu, Guan-Nan Tan, and Yong-Jin Zhou
School of Communication and Information Engineering, Shanghai University
Shanghai 200072, China

Abstract— This paper presents a wideband printed tapered slot antenna with pattern reconfigurability. The antenna consists of four tapered slots, a reconfigurable microstrip-to-slotline transition, and four PIN diodes. Four agile endfire radiation patterns are realized with the measured relative impedance bandwidth of 71.3%. The gains for the four directions are all higher than 6.4 dBi at the center frequency of 2.4 GHz. Good patterns are maintained at the four reconfigurable directions in a wideband. To further enhance the gain, the zero-index-metamaterial (ZIM) units are loaded in the tapered slot. The simulation results show that extra gains of 1.4 to 1.7 dBi can be obtained within the center band from 2.2 GHz to 2.6 GHz.

1. INTRODUCTION

Reconfigurable antennas with adjusting beams are demanded in the wireless communication systems such as small base stations. Adjusting beam antenna can provide pattern diversity, which results in improving signal to noise ratio and the capacity of the wireless communication systems. Planar printed antennas are preferred because of the low cost, low profile and easiness to be integrated with switches of PIN diodes and RF-MEMS.

Most of the reported pattern reconfigurable antennas have narrow bandwidth which could not satisfy the rapidly growing bandwidth requirement of the modern communication systems. In [1–3], broadband pattern reconfigurable monopoles antennas are proposed, and the relative bandwidths are 29%, 55.7% and 66.7%, respectively. However, there are only two or three reconfigurable radiation patterns and the gains are no more than 6 dBi. Ref. [4] presents a printed Yagi antenna with six adjustable beam directions. A tie-shape dipole with the two arms being printed on the opposite side of the dielectric-slab is adopted as the driven element to extend the bandwidth. Six PIN diode switches are attached between the ground and the driven dipole on the ground to control the radiation directions. The bandwidth of the reflection coefficient less than 10 dB is 400 MHz, and the gains are all 7.5 dBi on the six adjustable radiation directions.

Wideband pattern reconfigurable Vivaldi tapered slot antennas are proposed in [5–7]. Three different radiation patterns, including one omnidirectional and two endfire patterns are realized. The relative bandwidths are about 50% to 60% and the gains are less than 6.5 dBi. Most of the above mentioned designs include extra DC isolation structures, which add the complexity to the antennas.

In this paper, a broadband pattern reconfigurable tapered slot antenna is designed with four adjustable endfire directions. The antenna is coupling fed by a microstrip feedline. The four beam directions around 360° are controlled by four PIN diodes without extra bias circuits being required. This pattern reconfigurable antenna has wideband from 1.5 GHz to 3.3 GHz and high gain of 6.8 dBi at the center frequency of 2.4 GHz. The further approaches of gain enhancement are discussed by using zero-index metamaterial (ZIM).

2. PATTERN RECONFIGURABLE TAPERED SLOT ANTENNA

2.1. Antenna Structure

The antenna is printed on both sides of a square substrate with the relative permittivity of 2.65 and the depth of 0.8 mm. The side and top views are shown in Figs. 1(a) and (b). There are four metal sheets with the same sizes denoted as M_1, M_2, M_3 and M_4 on the top layer, which form four identical tapered slots denoted as S_1, S_2, S_3 and S_4. The antenna is fed by a 50 Ω microstrip line on the bottom layer, and the metal sheet M_1 acts as the ground plane.

Firstly, an original tapered slot antenna element with the length of L_s and the maximal slot width of W_{s2} is designed, whose bandwidth ($S_{11} < -10$ dB) is from 1.5 GHz to 3.3 GHz. A reconfigurable microstrip-to-slotline transition structure is elaborately designed to feed the four tapered slot radiators. Details of the transition dotted in Fig. 1(b) are enlarged in Fig. 1(c). It consists of

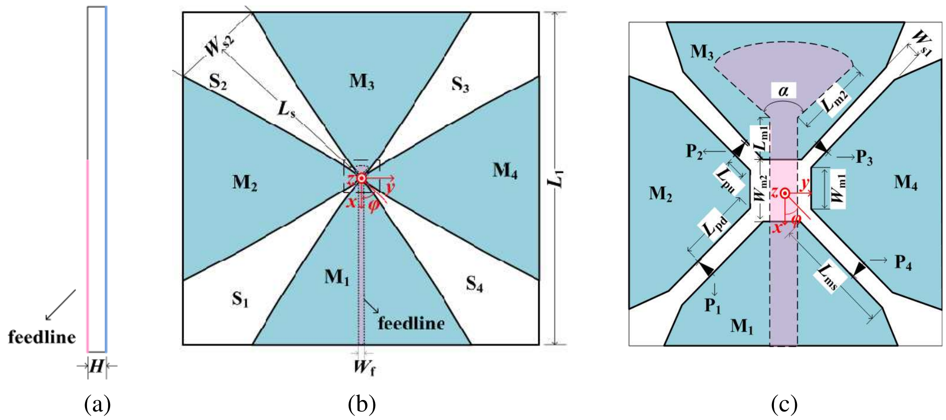

Figure 1: Antenna structure. (a) Side view. (b) Top view. (c) Detailed view.

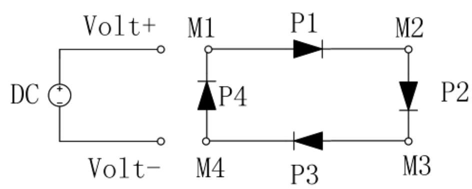

Figure 2: Schematic diagram of the bias circuit.

a microstrip feedline on the bottom layer, a square slot with the width of W_{m2} at the center on the top layer, and four rectangle slots with the length of L_{ms} and width of W_{s1}. The microwave on the microstrip line is coupled by the square slot, and then guided by four rectangles to the tapered slot radiators. A PIN diode is placed across each rectangle slot at an appropriate position. The dimensions are optimized using the software HFSS and the final sizes are (unit: mm): $H = 1.5\,\text{mm}$, $W_f = 4.1$, $W_{s2} = 83.6$, $L_s = 169.6$, $W_{s1} = 1.5$, $W_{m1} = 4.2$, $W_{m2} = 6.3$, $L_{ms} = 3.5$, $L_{m1} = 2.5$, $L_{pu} = 2.3$, $L_{pd} = 0.9$, $L_{m2} = 5.9$, $\alpha = 80^\circ$.

The selected PIN diode is Infineon BAR64-02V with the working frequency band from 0.1 GHz to 6 GHz. This diode can be equivalent to a resistance of $2.1\,\Omega$ on the forward-bias state and a capacitance of 0.17 pF on the reverse-bias one according to the datasheet. The polarities of the four PIN diodes are arranged clockwise as shown in Fig. 1(c). The simplified bias circuit is illustrated in Fig. 2. If one of the four tapered slots is chosen as the radiator, for example, S_1, the DC bias voltage should be added to the two adjacent metal sheets of M_1 and M_2. When one diode is on 'Off' state, the corresponding tapered slot radiates endfire pattern. At the same time, other three diodes are on 'On' state and the corresponding slots are shorted and do not work.

2.2. Simulation and Measurement Results

An antenna prototype with the bias circuit is fabricated and tested. The photograph of the fabricated prototype is shown in Fig. 3. Due to the symmetrical characteristic, the results of the directions of 315° and 225° chosen to be given here which are identified as 'down' and 'up' modes, respectively.

The reflection coefficients are measured by the Agilent 8722ES network analyzer The measured and simulated reflection coefficients are illustrated in Fig. 4. It can be seen that the measured common bandwidth of $S_{11} < -10\,\text{dB}$ is of both modes is from 1.57 GHz to 3.31 GHz and the relative bandwidth is 71.3%.

The simulated and measured normalized radiation patterns at the center frequency are illustrated in Fig. 5. It shows that the mainlobe directs to $\varphi = 315^\circ$ and $\varphi = 225^\circ$ in the xoy plane respectively. The measured cross polarization of the antenna is below 12 dBi at the mainlobe direction. The front to back ratio is more than 1 dBi at the center frequency.

3. GAIN ENHANCEMENT WITH ZIM

To enhance the antenna gain, the Zero-index metamaterial (ZIM) is designed. Meander-line resonator structure is chosen as the unit cell of the metamaterials which is shown in Fig. 6(a). The

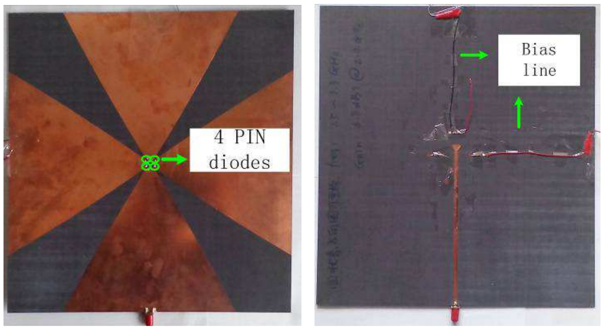

(a) (b)

Figure 3: Photograph of the proposed reconfigurable antenna. (a) Front view. (b) Bottom view.

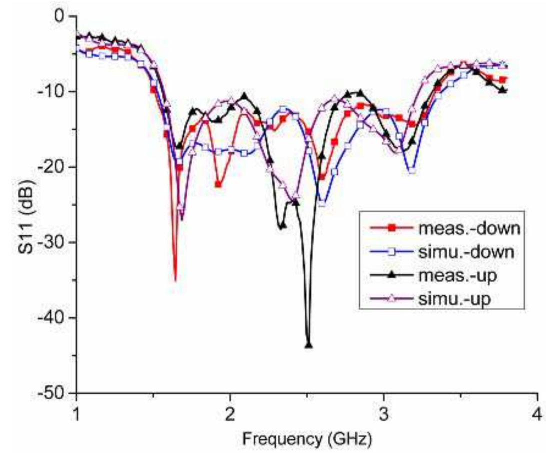

Figure 4: Simulated and measured reflection coefficient.

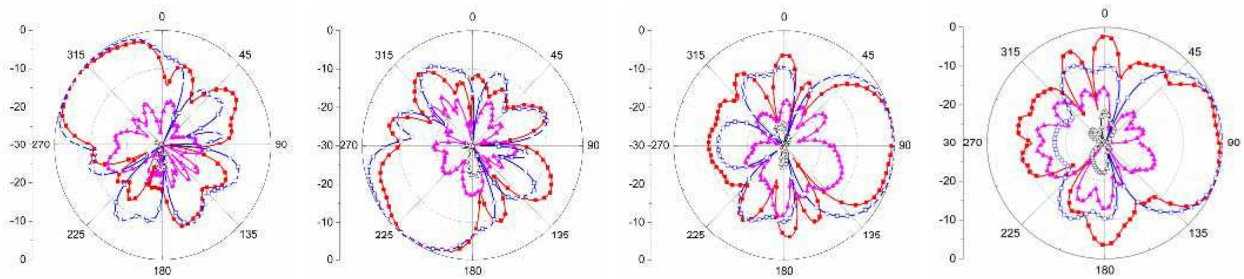

(a) (b) (c) (d)

Figure 5: Normalized radiation patterns at center frequency. (a) E plane of 'down' mode. (b) E plane of 'up' mode. (c) H plane of 'down' mode. (d) H plane of 'up' mode. (-■-: measured co-polarization; -▲-: measured cross-polarization; -□-: simulated co-polarization; -△-: simulated cross-polarization).

optimized dimensions are (in mm): $Lx = 13$, $Ly = 16$, $W = 0.8$, $Ax = 10.7$, $Ay = 1.2$. The effective permittivity and permeability are obtained using standard retrieval procedure, as shown in Fig. 6(b). It can be seen that the effective permittivity is about zero at around the 2.4 GHz. The bandwidth of $|\text{Re}(\varepsilon)| \leq 1$ is from 2.2 GHz to 2.8 GHz.

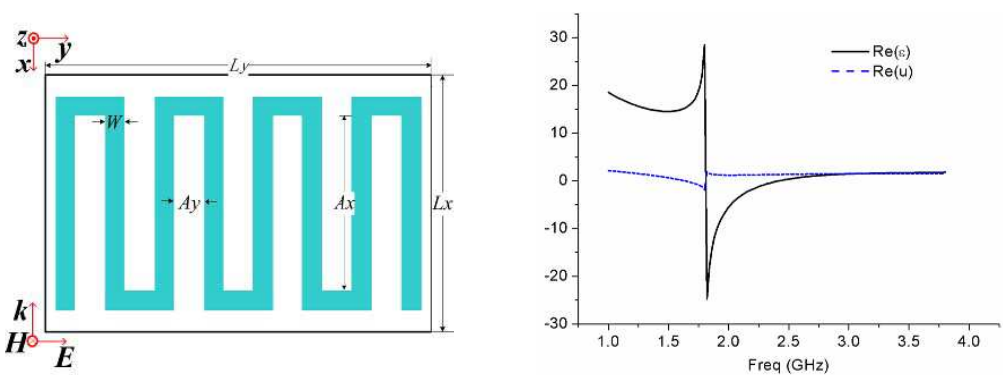

(a) (b)

Figure 6: Meander-line unit cell. (a) Structure and dimensions. (b) Retrieved results of the permittivity and permeability.

The ZIM unit cells are added to the tapered slots of the proposed antenna as shown in Fig. 7(a). The field distribution of the down mode at 2.4 GHz without and with ZIM is shown in Figs. 7(b) and (c), respectively. It can be seen that the field are mainly distributed in the slot S_1 on both cases. The ZIM cells make the field distribution more uniform than the antenna without ZIM,

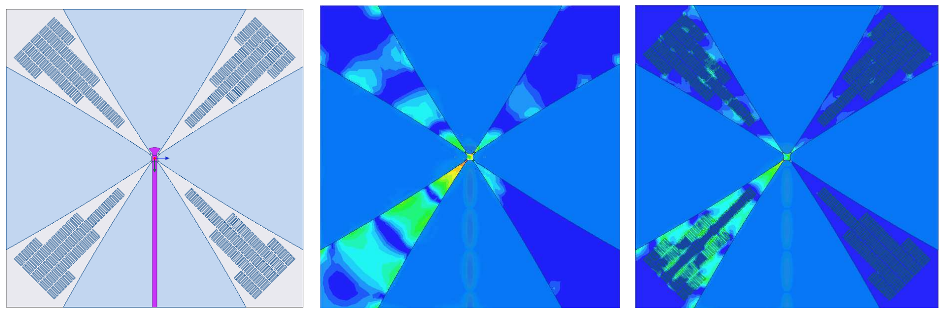

(a) (b) (c)

Figure 7: Antenna with ZIM. (a) Layout. (b) Field distribution at 2.4 GHz (a) without zim and (b) with ZIM.

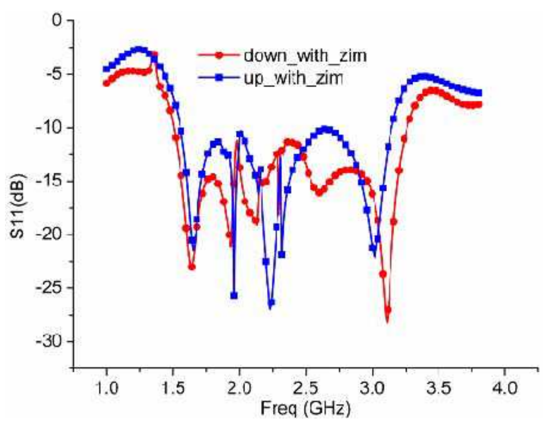

Figure 8: Simulated S_{11} of two directions with ZIM.

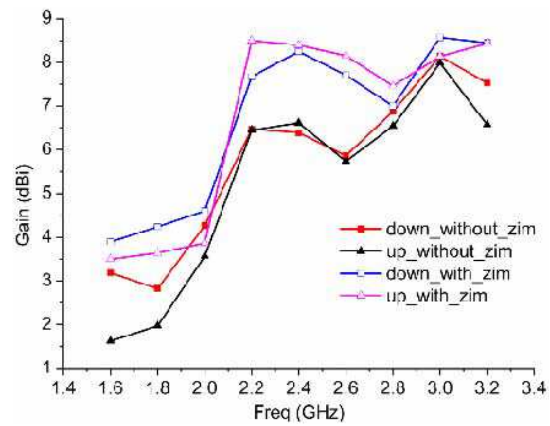

Figure 9: Gain response of two directions with and without ZIM.

which causes the gain enhancement. The reflection coefficients of both modes are illustrated in Fig. 8. Compared with Fig. 4, it can be seen that the impedance bandwidth of each directions are almost unchanged. The gain responses with and without the ZIM are compared in Fig. 9. The gains are improved about 1.4 to 1.7 dBi within the operation band from 2.2 GHz to 2.6 GHz. The gains with and without ZIM for the 'down' mode at the center frequency of 2.4 GHz are 8.2 dBi, and 6.6 dBi, respectively. Those for the 'up' mode are 8.4 dBi, and 6.4 dBi, respectively. A maximum improvement of 2 dBi has been obtained at the center frequency.

4. CONCLUSIONS

A novel wideband printed pattern reconfigurable antenna based on tapered slots is proposed. The antenna can switch its maximum radiation directions among four endfire directions within a broad bandwidth from 1.57 GHz to 3.31 GHz. ZIM of meander-line unit cells are designed and loaded on the tapered slot for gain enhancement. The gains increase about 1.4 to 1.7 dBi in the operation band from 2.2 to 2.6 GHz. The gains high than 8.2 dBi are achieved for different modes of the reconfigurable antenna.

REFERENCES

1. Ding, X. and B. Z. Wang, "A novel wideband antenna with reconfigurable broadside and endfire patterns," *IEEE Antennas Wireless Propag. Lett.*, Vol. 12, 995–998, 2013.
2. Zhang, G. M., J. S. Hong, G. Song, et al., "Design and analysis of a compact wideband pattern reconfigurable antenna with alternate reflector and radiator," *IET Microw. Antennas Propag.*, Vol. 6, No. 15, 1629–1635, Dec. 2012.
3. Aboufoul, T., C. Parini, X. Chen, et al., "Pattern-reconfigurable planar circular ultra-wideband monopole antenna," *IEEE Trans. Antennas Propagat.*, Vol. 61, No. 10, 4973–4980, Oct. 2013.
4. Gong, B. and X.-X. Yang, "A planar printed Yagi antenna with adjustable beam," *Journal of Shanghai University (Natural Science)*, Vol. 20, No. 1, 83–91, 2014.

5. Wu, S. J. and T. G. Ma, "A wideband slotted bow-tie antenna with reconfigurable CPW-to-slotline transition for pattern diversity," *IEEE Trans. Antennas Propagat.*, Vol. 56, No. 2, 327–334, Feb. 2008.
6. Li, Y., Z. Zhang, J. Zheng, Z. Feng, and M. F. Iskander, "Experimental analysis of a wideband pattern diversity antenna with compact reconfigurable CPW-to-slotline transition feed," *IEEE Trans. Antennas Propagat.*, Vol. 59, No. 22, 4222–4228, Nov. 2011.
7. Zhang, G. M., J. S. Hong, B. Z. Wang, G. B. Song, and P. Li, "Design and time-domain analysis for a novel pattern reconfigurable antenna," *IEEE Antennas Wireless Propag. Lett.*, Vol. 10, 365–368, 2011.